ELSEVIER

Carbohydrate Polymers 48 (2002) 131–141

Carbohydrate Polymers

www.elsevier.com/locate/carbpol

Order in maize mutant starches revealed by mild acid hydrolysis

C. Gérard, P. Colonna, A. Buléon, V. Planchot*

INRA, BP 71627, 44316 Nantes cedex 03, France

Received 20 September 2000; revised 12 March 2001; accepted 21 March 2001

Abstract

Maize mutants starches cover a broad range of features with respect to apparent amylose content (1–63%), fine structure of amylopectin (short- to long-chain ratios), crystallinity level (19–48%) and polymorphic type (various proportions of A-, B- and V allomorphs). This study subjected starches from single and double maize mutants to mild acid hydrolysis (35 days) with 2.2 N HCl. The crystallinity of these starches before and after 12 days of mild hydrolysis was studied by X-ray diffractometry. The linear chain length distribution of amylopectin and residues was studied after debranching, followed by high-performance anion-exchange chromatography with pulsed amperometric detection. Regardless of amylose content or crystallinity level, starches with a predominant B-crystalline type were less susceptible to acid degradation than others, and initial rates of hydrolysis were lower for B-type than A-type starches. Changes in initial hydrolysis rate may have been due to defective crystallites and/or dangling chains. Branch points were more frequent in residual fractions of A-type starches (normal, *wxdu*) than in predominant B-type starch (*aewx*). Conversely, residual fractions of a pure B-type starch (*ae*) appeared to have no branch points, suggesting the involvement of apparent amylose in crystallites.

Keywords: Starch mutant; Maize; Acid hydrolysis; Crystallinity

1. Introduction

Starch is the most significant form of carbon stored in plants in terms of the amount biosynthesized, the universality of its presence among different plant species, and its economic importance. Basically, starch consists of two major biopolymers, amylose and amylopectin. Amylose is essentially a linear macromolecule composed of α-1 → 4-linked glucosyl units, whereas amylopectin is a branched macromolecule with α-1 → 6 branches on the α-1 → 4-linked glucosyl chains (Buléon, Colonna, Planchot & Ball, 1998). Starch granules are composed of ordered and disordered regions. Ordered parts are mainly based on the packing of double helices formed from short branches of amylopectin molecules (French, 1984). Most of these double helices are organized into semi-crystalline layers, giving the granule a so-called 'semi-crystalline structure.' Depending on their botanical origin, native starches display different diffraction patterns (Katz, 1930): an A-type for normal cereal starches and a B-type for tuber and high-amylose cereal starches. However, the organization of the starch granule is very complex. Despite several decades of investigation into starch ultrastructure, many questions remain unresolved, such as the respective contributions of amylose and amylopectin to crystallinity, the distribution of ordered and unordered areas within the granule or the size distribution of crystalline areas. Zobel (1988) considered six different reasons why amylose is separated from amylopectin in maize starch (A-type), but mixed with it in potato starch (B-type).

The study of starch hydrolysis by amylases or acid is a mean of improving our understanding of starch granule structure. The susceptibility of starch granules to degradation depends on their botanical origin (Kainuma & French, 1971; Leach & Schoch, 1961; Robin, Mercier, Charbonnière & Guilbot, 1974; Robin, Mercier, Duprat & Charbonnière, Guilbot 1975). Acid hydrolysis is performed either with sulfuric acid, producing Naegeli amylodextrins (Näegli, 1874), or with hydrochloric acid producing lintnerized starches (Lintner, 1886). Acid hydrolysis is considered to yield the crystalline resistant parts of the granule and thus allows an estimation of the easily degradable fraction or amorphous part of starch (Robin et al., 1974). B-type starches are usually less susceptible to acid hydrolysis than A-type ones (Kainuma & French, 1971; Robin et al., 1974; Robin et al., 1975). However, other reasons for starch susceptibility to acid have been reported, such as amylose content (Planchot, 1993) or the molar ratio of short to long chains (Biliaderis, Grant & Vose, 1981).

* Corresponding author. Fax: +33-240-67-51-67.
E-mail address: planchot@nantes.inra.fr (V. Planchot).

0144-8617/02/$ - see front matter
PII: S0144-8617(01)00219-3

It is difficult to design experiments conducive to meaningful analysis of the relationships between different structural levels and direct susceptibility to mild acid hydrolysis. The major difficulty is to obtain samples covering broader ranges of structural variations than the option of wild genotypes. Maize mutant starches are appropriate substrates since they are numerous (Nelson & Pan, 1995) and cover a broad range of granular and macromolecular structures. A previous study of the susceptibility of maize mutant starches to amylolysis enabled us to show that susceptibility decreased as the proportion of B-type crystallites increased (Gérard, Colonna, Buléon & Planchot, 2001c). It seemed likely that resistant regions were not strictly due to the presence of B-type crystallites, but rather to their arrangement and their influence on local organization, resulting in residual external shells (Gérard, Colonna, Bouchet, Gallant & Planchot, 2001b).

The main purpose of the present study was to show that maize mutations offer a means of broadening the range of starch behavior in response to mild acid hydrolysis and to evaluate the influence of crystallinity level and polymorphic type (A- to B-type ratio) on starch susceptibility to acid. The respective contributions of amylose and amylopectin to crystallinity were also investigated.

2. Experimental

2.1. Materials

2.1.1. Starch substrates

Several single and double maize mutant genotypes were used in this study: *waxy* (*wx*), *amylose extender* (*ae*), *dull* (*du*), *sugary-2* (*su2*), *aewx*, *aedu*, *dusu2* and *wxdu*. These samples were a gift from Limagrain Genetics (France). These starches were isolated industrially at a steeping temperature of around 50°C from maize harvested in 1995 in France and dried at 40–45°C. Normal maize starch was purchased from Roquette Frères (France).

2.1.2. Enzyme

Isoamylase (EC 3.2.1.68) of *Pseudomonas amyloderamosa* (59,000 UI/mg) was purchased from Hayashibara (1 mg/ml). All reagents were of analytical grade.

2.2. Methods

2.2.1. Determination of amylose content

Amylose content was determined with concanavalin A according to a procedure derived from (Gibson, Solah & McCleary, 1997). This method estimated an apparent amylose content corresponding to the proportion of α-glucans with few branches. Apparent amylose consisted of true amylose and part of the intermediate material (Gérard, Barron, Colonna & Planchot, 2001a). This intermediate material, composed of long linear chains and ramifications, was designated as IM2 (Gérard et al., 2001a). True amylose content was estimated by running size-exclusion chromatography on a HW75 S column (2.6 × 200 cm) using water as eluent (Gérard et al., 2001a).

2.2.2. Kinetics of mild acid hydrolysis

Native starches were suspended (20 g/l) in 2.2 N HCl. The containers were placed at 35°C, and the suspension was shaken daily to resuspend the sedimented granules (Robin et al., 1974). Aliquots (1 ml) were withdrawn at different time intervals and centrifuged for 10 min at 10,000*g*. Total solubilized sugars were measured in the supernatant by the orcinol-H_2SO_4 method (Planchot, Colonna & Saulnier, 1997), and the extent of degradation was expressed as the percentage of dry substrate solubilized. According to hydrolysis extents (HE) measured for the first two time intervals, initial hydrolysis rate was determined as the instantaneous rate $V_i = \Delta HE/\Delta t$ over the first days.

2.2.3. Preparation of crystalline residues

Crystalline residues of starches (lintners) were obtained by mild acid hydrolysis according to the aforementioned method. After 1, 2 or 12 days of hydrolysis, the remaining solid material was washed by successive centrifugations in distilled water until neutrality and then dried and stored at room temperature.

2.2.4. X-ray diffractometry

X-ray diffraction analyses were performed on native and degraded starches containing 20% H_2O (w.b.) after water sorption for ten days in desiccators under partial vacuum. Relative humidity was adjusted to 90% with a saturated $BaCl_2$ solution. The samples (20 mg) were then sealed between two tape foils to prevent any significant change in water content during measurement. Diffraction diagrams were recorded using Inel X-ray equipment operating at 40 kV and 30 mA. CuKα_1 radiation ($\lambda = 0.15405$ nm) was selected using a quartz monochromator. A curved position-sensitive detector (Inel CPS 120) was used to monitor the diffracted intensities during 2-h exposure periods. Relative crystallinity was determined after bringing all recorded diagrams to the same scale by normalization of total scattering between 3 and 30° (2θ), according to a method derived from (Gernat, Radosta, Damaschun & Schierbaum, 1990). A- and B-type recrystallized amyloses were used as crystalline standards after substraction of an experimental amorphous curve up to null intensity in regions without diffraction peaks. Extruded potato starch was used as the amorphous standard.

2.2.5. Isoamylase debranching of native starches

Starch (12.5 mg) was solubilized in 95% dimethyl sulfoxide (1 ml) for 3 days at room temperature under gentle magnetic stirring. To 80 μl of this solution were added 118 μl of pure water, 200 μl of citrate buffer (50 mM, pH 3.8), 2 μl of $CaCl_2$ (1 M) and 10 μl of isoamylase.

Table 1
The different variables of native starches examined with PCA

Variable	Description
Con A	Apparent amylose content determined with concanavalin A
SEC	Real amylose content determined with size exclusion chromatography
dp_{max}	Degree of polymerization of isoamylase debranched macromolecules with maximum area determined with HPAEC-PAD
S/L	Short to long chains ratio of debranched macromolecules determined with HPAEC-PAD (short: dp 7–20; long: dp > 20)
%Cryst	Crystallinity level
%A	Proportion of crystallites showing an A-type
%B	Proportion of crystallites showing a B-type
%V	Proportion of crystallites showing a V-type
V_i	Initial hydrolysis rate (%/day)
EDF	Easily degradable fraction (%)
HE	Final hydrolysis extent (%)

Debranching was then performed by 48-h incubation at 37°C in a water bath.

2.2.6. Isoamylase debranching of lintners

Lintners (5 mg) were solubilized in 1 M potassium hydroxide (100 μl) for 2 days at 4°C under gentle magnetic stirring, and 900 μl of pure water were then added. To 250 μl of this resulting solution (5 mg/ml) were added 0.1 M HCl (250 μl) and citrate buffer (50 mM, pH 3.8) (500 μl). Debranching was performed on 400 μl by addition of 5 μl of isoamylase and 48-h incubation at 45°C in a water bath.

2.2.7. Branched chain length distribution

Branched chain length distributions of native starches after isoamylase debranching as well as lintners before and after isoamylase debranching were analyzed using high-performance anion-exchange chromatography with a pulsed amperometric detector system (HPAEC-PAD). Debranched samples (1.25 or 2.5 mg/ml) were filtered on 0.45 μm, and an aliquot (20 or 10 μl) was injected onto a CarboPac PA-100 anion-exchange column (250 × 4 mm) coupled to a CarboPac PA-100 guard column. The acetate gradient system included two eluents: 150 mM NaOH (eluent A) and 150 mM NaOH containing 600 mM NaOAc (eluent B). The flow rate was 1 ml/min. The elution gradient was (i) 0–8 min with 100% eluent A, (ii) 8–9 min with a linear gradient from 0 to 25% eluent B, (iii) 9–24 min with a second linear gradient to 45% eluent B, (iv) 24–49 min with a third linear gradient to 57.5% eluent B, (v) 49–54 min with a fourth linear gradient to 100% eluent B, (vi) 54–59 min with 100% eluent B, (vii) 59–64 min with a linear gradient to 100% eluent A, and (viii) 64–84 min with 100% eluent A. The short- to long-chain ratio (*S/L*) was estimated as

$$S/L = \sum_{i=7}^{i=20} \%\text{area} / \sum_{i=21}^{i=50} \%\text{area}$$

where $\sum_{i=7}^{i=50} \%\text{area} = 100$ and i is the degree of polymerization (dp). In HPAEC-PAD, as response coefficients decreased with increasing dp, the % area of long chains underestimated its true proportion. However, as the underestimation was similar for all samples, peak areas could be used to compare *S/L* ratios.

2.2.8. Statistical analysis

Principal component analysis (PCA) was performed on the data set, using AnaMul™ software (INRA, France). The variables were the apparent amylose content (ConA), true amylose content (SEC), degree of polymerization with maximum area (dp_{max}), short- to long-chain ratio (*S/L*), crystallinity level (%Cryst), proportion of A-, B- and V-type crystallites (*%A*, *%B* and *%V*, respectively), initial hydrolysis rate (V_i), easily degradable fraction (EDF) and final hydrolysis extent (HE) (Table 1). The observations were the samples.

3. Results — discussion

3.1. Substrate characteristics

The amylose contents of starches from maize mutants were determined by size exclusion chromatography (SEC) and complexation with concanavalin A. In previous work (Gérard et al., 2001a), we demonstrated that starch biosynthesis without some of the enzymes involved in granule construction produces a polysaccharide different from amylopectin and amylose. This polysaccharide shows an intermediate structure between the two well-known starch macromolecules (IM2, for intermediate material 2), which creates difficulties for the amylose assay. The apparent amylose content of starch samples was determined by a concanavalin A procedure that estimated the ratio of linear to branched macromolecules. This population include amylose and branched macromolecules with long external chains length from IM2. These apparent amylose contents ranged from less than 1% in *wx* starches to 63% in *ae* starch, whereas true amylose contents (estimated by SEC) ranged from less than 1% (*wx*) to 54% (*ae*) (Table 2). As a part of intermediate material 2 was included, apparent amylose values were higher than those for true amylose (Gérard et al., 2001a). After isoamylase debranching, all native starches showed a bimodal distribution, with the maximum area for degree of polymerization (dp_{max}) ranging from 11 (*su2*) to 15 (*ae*, *aewx*) (Table 2). Branched macromolecules showed different fine structures since the short- to long-chain ratio ranged from 1.9 for *ae* starch to 4.3 for *su2* starch (Table 2). The relationship between amylopectin average chain length ($\overline{CL}$) and polymorphic type for 20 different

Table 2
Structural features and hydrolysis parameters of native starches (nd: not detected)

	Apparent amylose (%) [a]	True amylose (%) [b]	dp_{max} (% area)	S/L [c]	Crystallinity level (±4%)	A-type (%)	B-type (%)	V-type (%)	Initial rate (%/day)	EDF [d] (%)	Final hydrolysis extent (%)
wx	nd	Nd	12	3.6	48	100	0	0	14	58	95
wxdu	nd	nd	12	3.5	44	100	0	0	16	67	95
Normal	24	26	12	3.8	31	100	0	0	14	51	90
Su2	50	24	11	4.3	19	15	15	70	29	56	90
Du	45	27	12	3.9	28	70	10	20	14	59	85
dusu2	58	34	12	4.2	24	35	20	45	24	57	80
aedu	56	30	12,14	2.8	28	25	45	30	13	50	80
aewx	7	nd	15	2.1	47	25	75	0	11	46	75
Ae	63	54	15	1.9	30	0	100	0	7	36	60

[a] Determined with Concanavalin A.
[b] Determined with size exclusion chromatography.
[c] Estimation of short to long chains ratio in starch.
[d] Easily degradable fraction.

starches from various botanical sources was previously studied by Hizukuri (1985), who found a $\overline{CL}$ increase in B-type starches. Moreover, in vitro studies showed an A-type diffraction diagram for glucose chains with degrees of polymerization (dp) of 10–12, and a B-type for higher degrees (Pfannemüller, 1987). Quantitative results could not be obtained from HPAEC-PAD in the present study. However, the dp_{max} value was higher as the proportion of B-type crystallites in starch increased (Tables 1 and 2), which is in agreement with Hizukuri's rule. Starch granules showed equivalent average diameters of around 8 μm (data not shown). According to multilinear regression performed on diffracted intensities, maize mutant starches covered a wide range of crystallinity levels, ranging from 19% in *su2* starch to 48% in *wx* starch, with most of the values between 24 and 31% (Table 2). Starches displayed four different X-ray diffraction patterns (Table 2). *Du*, *su2*, *dusu2* and *aedu* starches showed complex diffractograms since they contained various amounts of A, B and V crystalline types. The V-crystalline type was never detected in native maize mutant starches and was probably induced by a steeping temperature (50°C) too high for the kernels. This artifact was checked by running X-ray experiments on *su2* flours before and after a steeping step at 50°C for 24 h (data not shown). *aewx* starch displayed a C-type diffractogram, with 25 and 75% of A- and B-types, respectively; *ae* starch was pure B-type; and normal, *wx* and *wxdu* starches were pure A-type.

3.2. Hydrolysis kinetics

The wide ranges of hydrolysis kinetics and final extents observed were not attributable to different specific granule areas since all starches studied had equivalent average diameters. Hydrolysis curves, plotted as a semi-logarithmic form $[\log(100/100 - X)]$ where X is hydrolysis extent (Robin et al., 1974) vs time, showed two first-order kinetics (Fig. 1) indicative of the varying behavior of acid on two different structural organizations: a first rapid stage during which amorphous layers within the starch granule are assumed to be eroded and a second slower stage in which crystallites are degraded (Kainuma & French, 1971; Robin et al., 1974).

The first stage was characterized by hydrolysis rates ranging from 7 to 29%/day according to the starch genotype (Table 2), and durations ranging from 4 to 10 days. Among the tested starches, *su2* and *dusu2* samples showed very high hydrolysis rates (29 and 24%/days, respectively) with short first phases (~4–5 days) compared to the other starches for which this phase was longer. High initial hydrolysis rates were previously reported for *su2* and *dusu2* starches during enzymatic hydrolysis by porcine pancreas α-amylase (Gérard et al., 2001c) and for *sugary-2 opaque-2* (*su2o2*) starch during acid hydrolysis (Inouchi, Glover & Fuwa, 1987).

Normal, *wx*, *du* and *su2* starches showed final hydrolysis

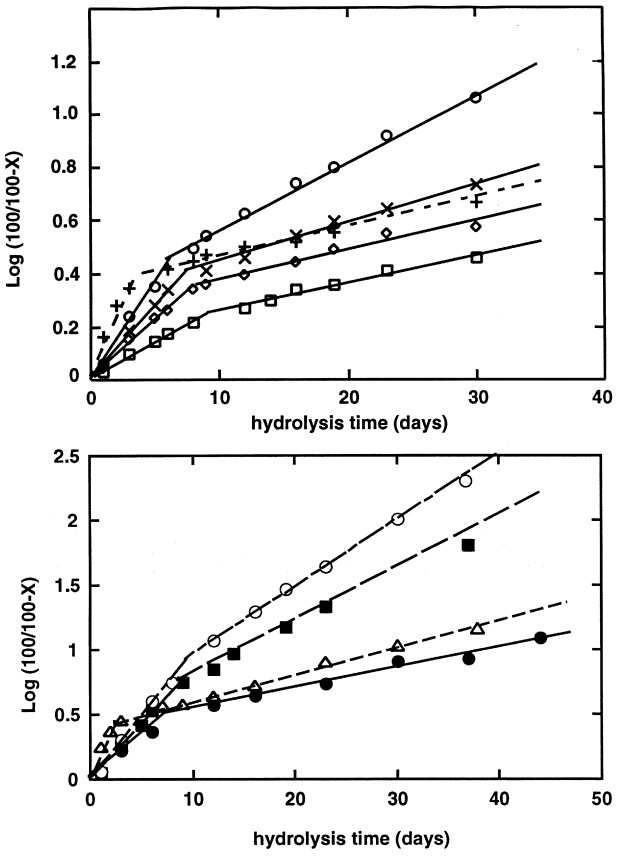

Fig. 1. Mild acid hydrolysis kinetics (2.2 N HCl,35°C) of various maize starch granules plotted as a logarithmic form. (a) —○— normal, —×— *aedu*, - + - *dusu2*, —◇— *aewx*, and —□— *ae*. (b) —○— *wxdu*, —■— *wx*, —△— *su2* and —●— *du* (X: hydrolysis extent).

extents above 85%, and *aewx*, *aedu* and *dusu2* double maize mutants starches showed intermediate hydrolysis extents of 75–80%. It is generally considered that high-amylose maize starches show low susceptibility to mild acid hydrolysis, whereas those with low amylose are highly degraded (Kainuma and French, 1971; Robin, 1976). According to final hydrolysis extents (Table 2), *ae* starch showed quite low susceptibility to mild acid hydrolysis (60%), whereas *wx* and *wxdu* starches displayed the highest hydrolysis extents (95%), in agreement with previous observations. However, a low-amylose starch (7%) such as *aewx* appeared to be less susceptible to mild acid hydrolysis than normal, *du* and *su2* starches (24, 45 and 50% apparent amylose, respectively). Moreover, some of the high-amylose starches tested (*aedu* or *dusu2*) were more susceptible than *ae* starch. These observations are consistent with the work of Inouchi et al. (1987) who found that high-amylose starches [*su2o2* and *duo2*(*dull opaque-2*)] are highly susceptible to acid. Thus, despite the low susceptibility of high-amylose starch to acid hydrolysis and the high susceptibility of *wx* starch, amylose and hydrolysis parameters were not closely related. Biliaderis et al. (1981) also reported that amylose content was not correlated with the initial rate of acid hydrolysis for legume starches.

The actual paradigm is that acid degrades amorphous regions preferentially. However, in the present work, no close relation was found between hydrolysis parameters and relative crystallinity. This is illustrated by *wxdu* and *aewx* starches, both of which showed similar high crystallinity levels (44 and 47%, respectively), but different initial hydrolysis rates (16 and 11%/days) and final hydrolysis extents (95 and 75%). Normal, *du*, *aedu* and *ae* starches also displayed similar crystallinity levels (~30%) and different hydrolysis parameters. Moreover, *wx*, *wxdu*, normal and *su2* starches showed different crystallinity levels (48, 44, 31 and 19%, respectively) and were all nearly completely degraded (>90%) in our experimental conditions.

This absence of correlation between crystallinity level and susceptibility to acid was confirmed by extrapolation of the second stage (Fig. 1) to null time, which allowed the easily degradable fraction (EDF) of starch to be estimated (Robin et al., 1975). EDF values ranged from 36 to 67% depending on the genotype considered (Table 2). EDF (supposedly the amorphous part) was greater for a normal (51%) than a high-amylose starch (36%), though the samples showed equivalent crystallinity levels (30%). Moreover, *wx*, *du* and *dusu2* starches showed similar EDF values (~57.5 %) despite different crystallinity levels (48, 28 and 24%, respectively). Indisputably, mild acid hydrolysis allowed crystalline residues to be isolated, although all these observations clearly demonstrated that crystallinity level had no direct influence on the intrinsic acid-induced behavior of starch to hydrolysis.

A clear relationship was found between hydrolysis parameters and the amount of B-type crystallites, i.e. starch susceptibility to acid was lower and the number of residual structures greater as the amount of B-type crystallites increased. This phenomenon was apparent for the amount of B-type crystallites in the whole granule relative to the amount of residual material (Fig. 2), for which a quite good correlation was found (dotted line), with a slope close to 1. Residual structures are likely to be composed solely of B-type crystallites (single line), thereby confirming that B-type crystallites within the starch granule constitute an intrinsic limitation to acid degradation.

3.3. X-ray diffractometry on native and hydrolyzed starches

Residues were compared after first-stage erosion. The crystallinity of residual fractions was determined on normal, *ae*, *aewx*, *aedu*, *dusu2* and *wxdu* starches after 12 days of hydrolysis, when hydrolysis extents were 78, 43, 64, 64, 74 and 85%, respectively. The behavior of V-type in the first stage of hydrolysis was also noteworthy: X-ray analyses were performed on *dusu2* and *aedu* starches (containing 45 and 30% of crystallites with a V-type, respectively) after 1 and 2 days of hydrolysis, respectively, when hydrolysis extents were 42 and 37% for *dusu2* and *aedu*, respectively.

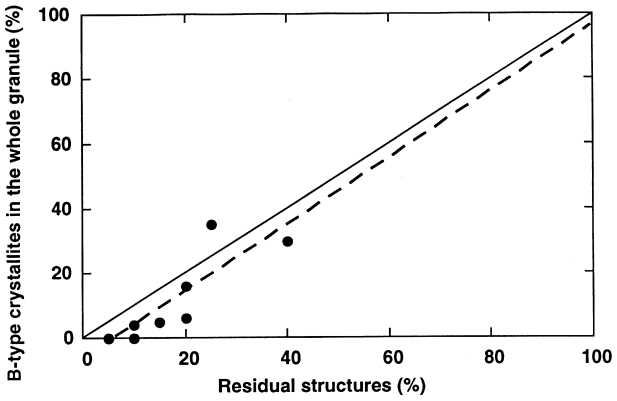

Fig. 2. Amount of B-type crystallites in the whole granule versus the proportion of residual structures (%) after acid hydrolysis for the various maize starches. (dotted line: experimental correlation; single line: theoretical correlation, if residual structures were only composed of B-type crystallites).

A clear increase in crystallinity level was observed for all starches treated with acid, as indicated by the higher diffracted intensities (Fig. 3). Acid degraded amorphous layers preferentially, regardless of the structural organization. With respect to polymorphic types, no significant changes were detected after hydrolysis in starches showing either a pure A-type (normal and *wxdu*) or a predominant B-type (*ae*, *aewx*). Conversely, for starches showing a complex A- B- and V-type (*aedu*, *dusu2*), V-type crystallites were preferentially degraded by acid, and the B-type proportion was significantly increased as soon as hydrolysis began (Fig. 3). V-type degradation was revealed by the disappearance of the 19.9° reflection, specific for the V-type (bold arrow). Consequently, residual hydrolyzed starches displayed a C-type with a higher proportion of B-type crystallites. As the amount of residual structures (almost solely B-type) was consistent with the initial amount of B-type crystallites in the whole granule (Fig. 2), B-type crystallites were intrinsically resistant to acid degradation.

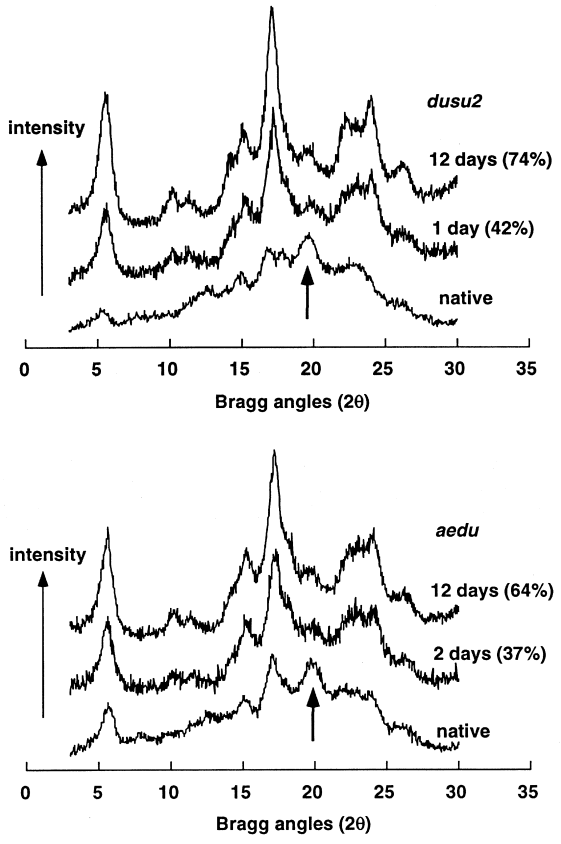

Fig. 3. X-ray diffraction patterns of *dusu2* and *aedu* starches before and after various hydrolysis times. Hydrolysis extents are indicated in brackets.

3.4. Chain length distribution of native and hydrolyzed starches

Our purpose was to compare constitutive chains of residues, which are supposedly in crystallite form after first-stage erosion. Chain length distribution of residual fractions before and after isoamylase debranching was determined for all starches after 12 days of hydrolysis. Figs. 4 and 5 show the behavior of A- or B-types and high-amylopectin or high-amylose starches, showing chain length distributions of normal (Fig. 4a), *wxdu* (Fig. 4b), *ae* (Fig. 5a) and *aewx* (Fig. 5b) lintners before and after isoamylase debranching. Hydrolysis extents of normal, *wxdu*, *ae*, and *aewx* starches after 12 days of acid hydrolysis were 78, 85, 43 and 64%, respectively. For A-type starches (normal, *wxdu*), lintners showed a bimodal distribution, with a first population of maximum area (dp_{max}) for dp 13, and a second population of dp_{max} 21 and 26 for normal and *wxdu* samples, respectively. After isoamylase debranching, these A-type lintners showed a single distribution with a dp_{max} of 13 (Fig. 4). Therefore, normal and *wxdu* starches, after 78 and 85% of hydrolysis, respectively, consistently retained a substantial proportion of single-branched molecules with dp_{max} of about 21 and 26, respectively, that were hydrolyzed into two linear molecules after isoamylase debranching. These results are in agreement with those reported for lintners (Robin et al., 1974) and for Naëgeli dextrins (Jane, Wong & McPherson, 1997) from normal and *waxy* maize starches. For predominant B-type starches (*ae*, *aewx*), lintners also showed a bimodal (though less distinct) distribution, with a dp_{max} of 16 (Fig. 5). After isoamylase debranching, *aewx* showed a single distribution with the same dp_{max} (Fig. 5b), whereas *ae* still displayed a bimodal distribution (Fig. 5a).

A-type residues were composed of many branch points, which is consistent with the numerous chains in organized A-type clusters and the densely packed structure of A-type crystallites (Imberty, Chanzy, Perez, Buléon & Tran, 1987). Branch points and therefore amylopectin molecules are involved in A-type crystallites. *aewx* hydrolysis residues were composed of fewer branch points, which is consistent with reported observations (Jane et al., 1997) as well as with the presence of fewer branch points in native *aewx*

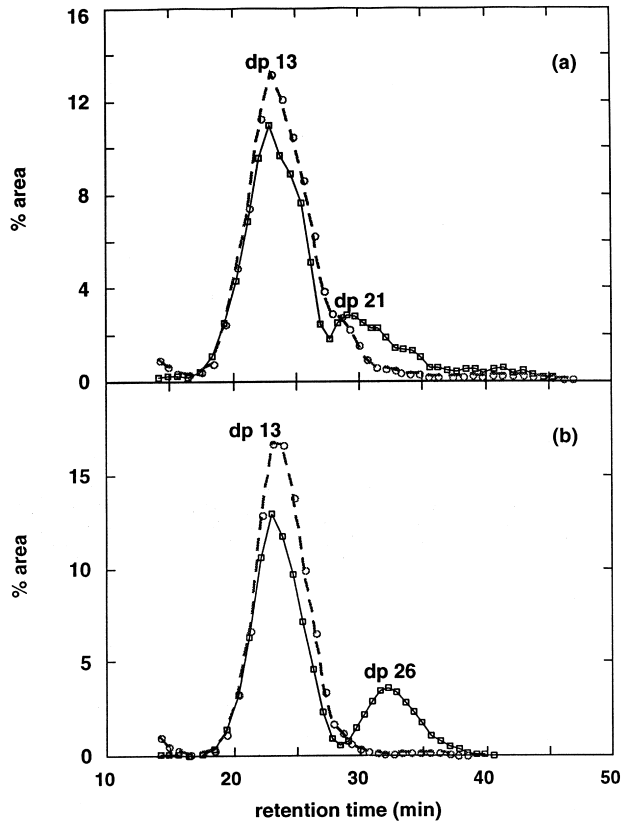

Fig. 4. HPAEC-PAD analysis of chain length distribution (% area) of residues after 12 days of acid hydrolysis (2.2 N HCl, 35°C) for (a) normal (78% hydrolysis) and (b) *wxdu* (86% hydrolysis) maize starches before (-⊟-) and after (-⊖-) isoamylase-debranching.

amylopectin (Fuwa, Glover, Miyaura, Inouchi, Konishi & Sugimoto et al., 1987; Yuan, Thompson & Boyer, 1993; Gérard, Planchot, Colonna & Bertoft, 2000) and the less packed structure of B-type crystallites (Imberty & Perez, 1988). Consequently, substantial branch (α-1,6) linkages of A-type starch were located within the crystalline region and others in the amorphous region, as reported by Jane et al. (1997). For B-type starch, most of the branch linkages could rather be clustered in the amorphous region, and thus more susceptible to acid hydrolysis (Jane et al., 1997). However, in the absence of any evaluation of the original branch points in native starches, it cannot be concluded that there were fewer branch points in B-type than A-type residues. It is possible that native B-type starch is composed of fewer chains, which would mean that hydrolysis residues have fewer branch points than in the case of A-type starches.

3.5. Principal component analysis (PCA)

The variables for PCA were apparent amylose content (ConA), true amylose content (SEC), degree of polymerization with maximum area (dp_{max}), the short- to long-chain ratio (*S/L*), crystallinity level (%Cryst), proportion of A-, B- and V-type crystallites (*%A*, *%B* and *%V*, respectively), initial hydrolysis rate (V_i), easily degradable fraction (EDF) and final hydrolysis extent (HE) (Table 1). The first and second principal components (PC), accounting for 66% and 25% of variance respectively, provided an overview of the starch samples (Fig. 6). Normal, *wx* and *wxdu* starches had high positive scores in PC1, whereas *ae* starch had a high negative score (Fig. 6a). The two *ae* and *aewx* starches had negative scores in PC2, whereas all other samples had positive ones. The two *su2* and *dusu2* mutant starches had very high positive scores in PC2, showing a strong influence of this component. The starches from *su2*, *dusu2*, *aedu* and *aewx* mutants were close to PC2, indicating little influence of PC1.

The loading plot (Fig. 6b)) for the first two PC accounted for 91% of the variance in structural and hydrolysis variables. The close relation of variables in pairs or groups indicated that the correlation was positive. The pair of variables describing %B and dp_{max} confirmed previous findings that high dp_{max} favors B-type crystallization (Gidley, 1987; Pfannemüller, 1987). ConA and SEC, though determining different structural macromolecules, were also positively correlated (0.92), indicating that the amount of intermediate material (IM2) becomes greater as amylose content increases. The variables describing *%V*, V_i and *S/L* were positively correlated since they had high scores in PC2. In addition, HE and EDF were negatively correlated with *%B* since these variables were found on the opposite side of a diagonal (intersecting zero point) in the plot. Similarly, %Cryst was negatively correlated with *%V*, SEC and ConA. Variables found in orthogonal directions, as indicated by the arrows in Fig. 6, varied independently of each other. Thus, ConA, SEC, *%V* and %Cryst varied independently of variables describing the hydrolysis parameters (EDF, HE) and *%B* (Fig. 6).

When scores and loading plots were compared (Fig. 6), normal, *wx* and *wxdu* starches showed high positive scores in PC1 as their proportions of A-type crystallites, hydrolysis extent and easily degradable fraction were all high. Similarly, *ae* starch had a high negative score in PC1 due to a high proportion of B-type crystallites. The two *su2* and *dusu2* mutant starches had positive scores in PC2, corresponding to high proportions of V-type crystallites, high *S/L* ratios and high initial hydrolysis rates. Finally, *ae* and *wxae* starches had negative scores in PC1 and PC2 because of their low hydrolysis extents and high B-type proportions.

3.6. Relationship between structural and hydrolysis parameters

PCA revealed that final hydrolysis extent and EDF value were negatively correlated with the proportion of B-type crystallites. The same negative correlation was previously reported for the susceptibility of maize mutant starches to enzymatic hydrolysis (Gérard et al., 2001c). Thus, the negative influence of B-type crystallites was associated with the formation of resistant B-type regions, which are

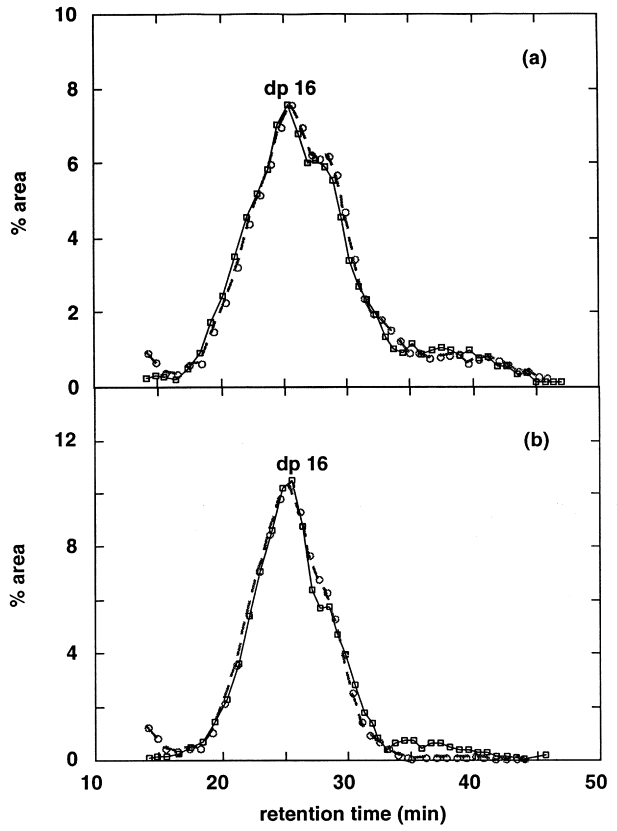

Fig. 5. HPAEC-PAD analysis of chain length distribution (% area) of residues after 12 days of acid hydrolysis (2.2 N HCl, 35°) for (a) *ae* (43% hydrolysis) and (b) *aewx* (64% hydrolysis) maize starches before (-⊟-) and after (-⊖-) isoamylase-debranching.

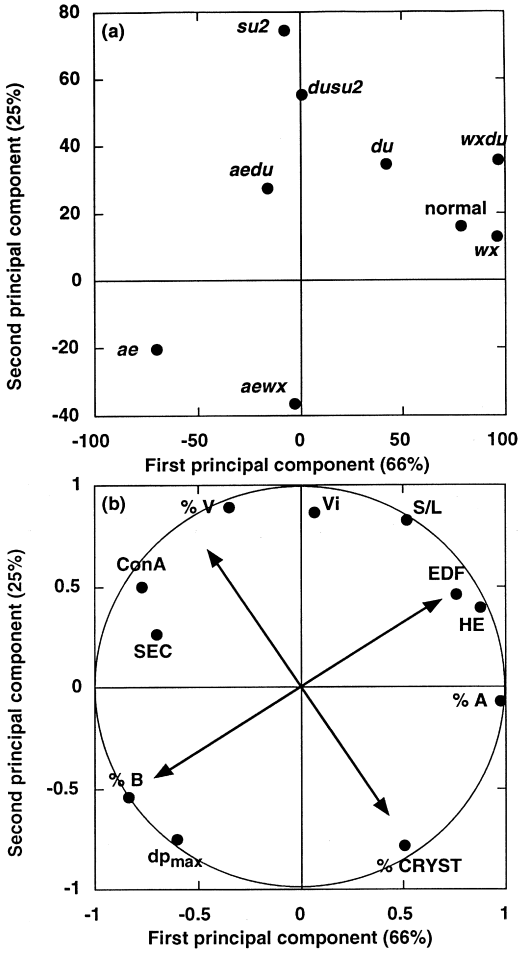

Fig. 6. Score plot (a) and loading plot (b) of principal components 1 and 2, describing the variation of the samples. Arrows indicate main trends in correlations between the different variables

considered to be composed of amorphous and crystalline material and supposedly arranged in a peripheral ring of starch granules that acts as a barrier to hydrolytic enzymes (Gérard et al., 2001c). As H_3O^+ ions (contrary to α-amylase) can diffuse easily within the granule, this organization cannot account for the behavior of maize starches to acid hydrolysis nor the negative correlation between B-type crystallites and final hydrolysis extent or EDF values. As acid hydrolysis is likely to isolate B-type crystallites, their resistance may result from intrinsic stability, three-dimensional size, their size along the *c*-axis, or a greater perfection as compared to A-type crystallites as already suggested (Planchot, Colonna & Buléon, 1997).

The initial hydrolysis rate was correlated with the proportion of V-type crystallites. Moreover, X-ray experiments showed that V-type crystallites were degraded as soon as hydrolysis began, i.e. at day 1 for *dusu2* starch and at day 2 for *aedu* starch (Fig. 3). Therefore, starches (*su2* and *dusu2*) showing very high initial rates (29 and 24%/day, respectively) displayed the highest V-type proportions (70 and 45). As V-type crystallites usually do not exist in native starches (Buléon et al., 1998) and were induced in this case by a steeping temperature too high for kernels, they were probably defective and/or highly susceptible to acid. Consequently, high initial hydrolysis rates could have been related to the large proportion of these defective crystallites that were rapidly degraded. The presence of V-type structures indicates that these starches were intrinsically more susceptible to forming complexes, i.e. chains were more available and consequently less resistant to acid. The initial hydrolysis rate was also correlated with *S/L* ratios, as previously reported for some legume starches (Biliaderis et al., 1981). As *su2* and *dusu2* starches displayed the highest *S/L* ratios (4.3 and 4.2), their high initial hydrolysis rates could have been due to the high proportion of very short chains in these starches, as revealed by HPAEC-PAD performed on native debranched starches (data not shown). Moreover, various authors have reported an accumulation of dp 6–11 chains in branched macromolecules from genotypes showing a deficiency for soluble starch synthase II (SSS II) activity, such as *su2* in maize (Baker, Broglie, Cressman, Everard, Hines & Huang et al., 1999), *rug5* in pea (Craig, Lloyd, Tomlinson, Barber, Edwards & Wang et al., 1998), an antisense in potato (Edwards, Fulton, Hylton, Jobling, Gidley & Rössner et al., 1999; Lloyd,

Landschütze & Kossman, 1999), or *sta3* mutant in *Chlamydomonas* (whose amylopectin contained more dp 2–7 chains and fewer dp 8–50 chains (Fontaine, D'Hulst, Maddelein, Routier, Pépin & Decq et al., 1993). As these accumulated short chains are not stable in acid, their presence can be considered as an accumulation of dangling chains favoring very high initial hydrolysis rates.

3.7. Involvement of apparent amylose in crystallite

PCA revealed that crystallinity level and amylose content determined by SEC (or apparent amylose content determined by complexation with concanavalin A) were negatively correlated (0.88), which suggests that the presence of amylose (or apparent amylose) macromolecules did not increase order. This is consistent with the usual paradigm in which amylopectin is responsible for crystallinity, since *waxy* mutant starches were more crystalline and high-amylose starches were less crystalline. Zobel (1988) considered various reasons why amylose is separated from amylopectin in maize starches, but not in potato starch. For example, (i) hot water leaches amylose more readily from maize (50%) than from potato (20%) starch granules; (ii) substantial amylopectin contamination was observed in amylose leached from potato as compared to that from several cereal starches, including maize; and (iii) α-amylase attacks maize more readily than potato starch.

The fact that a 100% negative correlation between amylose content and crystallinity level was not observed in our study suggests the involvement of apparent amylose in crystallites. This involvement could exist preferentially in high-amylose starch, such as *ae* which showed a B-type. *ae* starch, which is solely composed of 37% amylopectin, showed a crystallinity level of $30 \pm 4\%$. In comparison, *aewx* starch, which displayed a predominant B-type (75%), was composed of 93% amylopectin and $47 \pm 4\%$ crystallites. Similarly, *wx* mutant, composed of 99% amylopectin, showed $44 \pm 4\%$ A-type crystallinity. Thus, in both *wx* and *aewx* starches, only a half-fraction of amylopectin molecules was organized enough to be involved in crystallites. If the same ratio is applied to *ae* starch, which is composed of 37% amylopectin, the crystallinity level should be only 19%, i.e. about 10% below the observed value (Table 2). This difference suggests that apparent amylose is involved in the crystallites for *ae* starch.

Zobel (1988) gave various arguments for the separation of amylose from amylopectin in maize (A-type) and its mixture with amylopectin in potato starch (B-type). Kasemsuwan and Jane (1994), who conducted a study of cross-linked starch using ^{31}P nuclear magnetic resonance, considered that amylose is located in close proximity to amylopectin in normal maize starch. We previously reported that amylopectin clusters involved in crystallites of native starch are composed of only a few chains (4 or 5) for B-type starch (*aewx*) (Fig. 7a), whereas those from A-type amylopectin (*wxdu*) are composed of more chains (~10–20) (Fig. 7b) (Gérard, Planchot, Colonna & Bertoft et al., 2000). Given this difference, one or two apparent amylose chains added to a cluster originally composed of 3 chains would induce the formation of a cluster with 4 or 5 chains. The newly constituted cluster could thus participate in crystallinity for B-type starch, and the role of apparent amylose in such a cluster is significant (Fig. 7c). Conversely, in the case of an A-type cluster, an added apparent amylose chain would not have any strong influence on A-type crystallization, in that the role of amylopectin conceals any apparent amylose contribution (Fig. 7d). Consequently, the involvement of apparent amylose in crystallites could be detected in B-type, but not A-type, crystallites.

The bimodal and single distributions observed respectively before and after residue debranching indicate that branch points were present in crystallites. However, HPAEC-PAD of *ae* hydrolysis residues showed a less distinct bimodal distribution similar to that observed after isoamylase debranching and consistent with findings for high-amylose starch (Robin, 1976). The lack of any significant difference after isoamylase debranching could mean that there are no branch points in *ae* residues. However, as these residues display high crystallinity level, they are actually composed of double helices. As these double helices are free of branch points, apparent amylose chains might be involved in crystallites, which would make it impossible to perform any debranching of the residues. This hypothesis gains support from the work of Bogracheva, Cairns, Noel, Hulleman, Wang & Morris et al. (1999) who reported that *rug5* and *r* mutant pea starches (composed of 43 and 65% amylose respectively) showed acid-resistant parts with a multi-modal distribution of chain lengths both before and after isoamylase debranching, whereas lintners from wild type and *rb*, *rug3*, *rug4* mutant pea starches with less than 35% amylose showed a double and single chain length distribution before and after isoamylase debranching.

All these observations indicate that apparent amylose could be involved in crystallites. This contribution of apparent amylose in ordered starch areas would be greater in high-amylose starches and detectable in B-type starches.

4. Conclusion

As previously reported for amylolysis by porcine pancreatic α-amylase, B-type starches in the present study proved less susceptible to acid hydrolysis. However, it is difficult to compare enzymatic and acid hydrolysis since the behavior of these two catalysts is very different. Acid hydrolyses amorphous parts preferentially, whereas enzyme hydrolyses both amorphous and crystalline parts concomitantly. Contrary to acid, α-amylase shows specificity for α-1,4 linkages and chain length of the substrate. Though the first step in amylolysis at a molecular level is assumed to be close to the acid hydrolysis mechanism, these two hydrolysis patterns are very different. Thus, the factor of

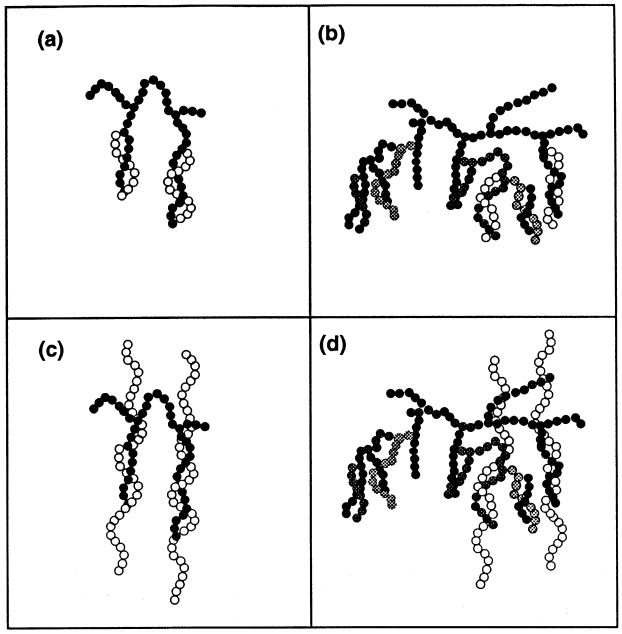

Fig. 7. Involvement of apparent amylose in crystallites: (a) a B-type cluster as an organized structure (after Gérard et al., 2000); double helices are composed of short chains from amylopectin, (b) an A-type cluster as an organized structure (after Nägeli, 1886); double helices are composed of short chains from amylopectin, (c) the presence of one or two apparent amylose chains (white circles) allows the B-type cluster to be involved in crystalline organization, (d) the presence of one or two apparent amylose chains (white circles) does not have a strong influence on A-type cluster crystallization.

susceptibility to amylolysis cannot be extrapolated to acid hydrolysis.

B-type crystallites could be intrinsically resistant to acid. Thus, residual structures might show increased crystallinity levels and B-type proportions because they are mainly composed of B-crystallites. Initial hydrolysis rates could depend on the amount of defective crystallites and the number of dangling chains that are too short to be involved in double helices. Contrary to previous assumptions, crystallinity levels and amylose contents were found to have no strong direct influence on susceptibility to acid hydrolysis.

Although amylopectin alone is assumed to be responsible for starch crystallinity, the study of the chain length distribution of crystallites showed that apparent amylose may be involved in crystallites. This involvement may concern B-type starches preferentially (whose amylopectin is composed of clusters with few chains) and be more significant in high-amylose starches.

Acknowledgements

This work was supported by the European Union FAIR Program "Genetic tailoring of novel starch polymers" (CT-95-0568). The authors are grateful to Mr Arnaud Messager from Ulice (France) for providing samples, and to Bruno Pontoire, Mélanie Hubert and Marie-Paule Pacouret for technical assistance.

References

Baker S., Broglie K., Cressman R., Everard J., Hines C., Huang C., Hubbard N., Lightner J., Marini M., & Pearlstein R. (1999). Modification of maize starch structure and functionality. *Genetic tailoring of novel starch polymers workshop*, September, Carry-le-Rouet, France.

Biliaderis, C. G., Grant, D. R., & Vose, J. R. (1981). Structural characterization of legume starches. II. Studies on acid treated starches. *Cereal Chemistry*, *58*, 502–507.

Bogracheva, T. Y., Cairns, P., Noel, T. R., Hulleman, S., Wang, T. L., Morris, V. J., Ring, S. G., & Hedley, C. L. (1999). The effects of mutant genes at the *r*, *rb*, *rug3*, *rug4*, *rug5* and *lam* loci on the granular structure and physico-chemical properties of pea starch. *Carbohydrate Polymers*, (39), 303–314.

Buléon, A., Colonna, P., Planchot, V., & Ball, S. (1998). Starch granules: structure and biosynthesis. *International Journal of Biological Macromolecules*, (23), 85–112.

Craig, J., Lloyd, J. R., Tomlinson, K., Barber, L., Edwards, A., Wang, T. L., Martin, C., Hedley, C. L., & Smith, A. M. (1998). Mutations in the gene encoding starch synthase II profoundly alter amylopectin structure in pea embryo. *Plant Cell*, *10*, 413–426.

Edwards, A., Fulton, D. C., Hylton, C. M., Jobling, S. A., Gidley, M., Rössner, U., Martin, C., & Smith, A. M. (1999). A combined reduction in activity of starch synthases II and III of potato has novel effects on the starch tubers. *Plant Journal*, (17), 251–261.

Fontaine, T., D'Hulst, C., Maddelein, M. -L., Routier, F., Pépin, T. M., Decq, A., Wieruszeski, J. -M., Delrue, B., Van den Koornhuyse, N., Bossu, J. -P., Fournet, B., & Ball, S. (1993). Towards an understanding of the biogenesis of the starch granule — Evidence that *Chlamydomonas* soluble starch synthase II controls the synthesis of intermediate size glucans of amylopectin. *Journal of Biology and Chemistry*, (268), 16 223–16 230.

French, D. (1984). In R. L. Whistler, J. N. Be Miller & E. F. Pashall, *Starch: chemistry and technology* (2nd ed). (pp. 183–247). Orlando, FL: Academic Press.

Fuwa, H., Glover, D. V., Miyaura, K., Inouchi, N., Konishi, Y., & Sugimoto, Y. (1987). Chain length distribution of amylopectins of double- and triple-mutants containing the waxy gene in the inbred Oh43 maize background. *Starch/Stärke*, (39), 295–298.

Gérard, C., Planchot, V., Colonna, P., & Bertoft, E. (2000). Relationship between branching density and crystalline structure of A- and B-type maize mutant starches. *Carbohydrate Research*, *326* (2), 130–144.

Gérard, C., Barron, C., Colonna, P., & Planchot, V. (2001a). Amylose determination in genetically modified starches. *Carbohydrate Polymers*, *44*, 19–27.

Gérard, C., Colonna, P., Bouchet, B., Gallant, D. J., & Planchot, V. (2001b). A multi-stage biosynthetic pathway in starch granules revealed by the ultrastructure of maize mutant starches. *Journal of Cereal Science*.

Gérard, C., Colonna, P., Buléon, A., & Planchot, V. (2001c). Amylolysis of maize mutants starches. *Journal of Science and Food Agriculture*,.

Gernat, C., Radosta, S., Damaschun, G., & Schierbaum, F. (1990). Supramolecular structure of legume starches revealed by X-ray scattering. *Stärke*, (42), 175–178.

Gibson, T. S., Solah, V. A., & McCleary, B. V. (1997). A procedure to measure amylose in cereal starches and flours with concanavalin A. *Journal of Cereal Science*, (25), 111–119.

Gidley, M. J. (1987). Factors affecting the crystalline type (A–C) of native starches and model compounds: a rationalisation of observed effects in terms of polymorphic structures. *Carbohydrate Research*, 301–304.

Hizukuri, S. (1985). Relationship between the distribution of the chain length of amylopectin and crystalline structure of starch granules. *Carbohydrate Research*, 295–306.

Imberty, A., & Pérez, S. (1988). A revisit to the three-dimensional structure of B-type starch. *Biopolymers*, (27), 1205–1221.

Imberty, A., Chanzy, H., Pérez, S., Buléon, A., & Tran, V. (1987). New three-dimensional structure of A-type starch. *Macromolecules*, (20), 2634–2636.

Inouchi, N., Glover, D. V., & Fuwa, H. (1987). Properties of residual maize starches following acid hydrolysis. *Starch/Stärke*, (39), 284–288.

Jane, J. L., Wong, K. S., & McPherson, A. E. (1997). Branch-structure difference in starches of A- and B-type X-ray patterns revealed by their Näegeli dextrins. *Carbohydrate Research*, *300*, 219–227.

Kainuma, K., & French, D. (1971). Näegeli amylodextrin and its relationship to starch granule structure. I. Preparation and properties of amylodextrins from various starch types. *Biopolymers*, (10), 1673–1680.

Kasemsuwan, T., & Jane, J. (1994). Location of amylose in normal starch granules. II Location of phosphodiester cross-linking revealed by Phosphorus-31 nuclear magnetic resonance. *Cereal Chemistry*, (71), 282–287.

Katz, J. R. (1930). Über die anderungen in Rontgenspektrum der stärke brim baker and beam altbacken warden des brutes. *Zeitschrift fur physikalische chemie*, (150), 37–59.

Leach, H. W., & Schoch, T. J. (1961). Structure of the starch granule. II Action of various amylases on granular starch. *Cereal Chemistry*, (38), 34–46.

Lintner, C. J. (1886). *Journal of Prakt. Chemistry*, *34*, 378.

Lloyd, J. R., Landschütze, V., & Kossman, J. (1999). Simultaneous antisense inhibition of two starch-synthase isoforms in potato tubers lead to accumulation of grossly modified amylopectin. *Biochemistry Journal*, (338), 515–521.

Nägeli, W. (1886). *Liebigs Annanlen der Chemie*, *173*, 218.

Nelson, O., & Pan, D. (1995). Starch synthesis in maize endosperm. *Annual Reviews in Plant Physiology and Plant Molecular Biology*, (46), 475–496.

Pfannemüller, B. (1987). Influence of chain length of short monodisperse amyloses on the formation of A- and B-type X-ray diffraction patterns. *International Journal of Biological Macromolecules*, (9), 105–108.

Planchot V. (1993). *Alpha-amylases d'Aspergillus fumigatus. Mécanismes d'action en phase hétérogène*. PhD Thesis, University of Nantes, France.

Planchot, V., Colonna, P., & Saulnier, Luc (1997). In B. Godon & W. Loisel, *Guide pratique d'analyses dans les industries des céréales* (pp. 350–353). Paris, France: Lavoisier.

Robin JP. (1976). *Comportement du grain d'amidon à l'hydrolyse acide ménagée. Etude physico-chimique et enzymatique de la fraction insoluble. Contribution à la connaissance de la structure de l'amylopectine*. PhD Thesis, University of Paris VI, France.

Robin, J. P., Mercier, C., Charbonnière, R., & Guilbot, A. (1974). Lintnerized starches Gel filtration and enzymatic studies of insoluble residues from prolonged acid treatment of potato starch. *Cereal Chemistry*, *51*, 389–406.

Robin, J. P., Mercier, C., Duprat, F., Charbonnière, R., & Guilbot, A. (1975). Amidons lintnérisés — Etudes chromatographiques et enzymatiques des résidus insolubles provenant de l'hydrolyse chlorhydrique d'amidons de céréales, en particulier de maïs cireux. *Die Stärke*, 36–45.

Yuan, R. C., Thompson, D. B., & Boyer, C. D. (1993). Fine structure of amylopectin in relation to gelatinization and retrogradation behavior of maize starches from three wx-containing genotypes in two inbred lines. *Cereal Chemistry*, (70), 81–89.

Zobel, H. F. (1988). Molecules to granules: a comprehensive starch review. *Starch/Stärke*, *40*, 44–50.